Electronic Supplementary Material (ESI) for Journal of Materials Chemistry C.
This journal is © The Royal Society of Chemistry 2016

Supplementary materials for

A two-dimensional cobalt(II) network with the remarkable positive axial anisotropy parameter exhibiting field-induced single-ion magnet behavior

Lin Sun,‡[a] Sheng Zhang,‡[a,c] Sanping Chen,*[a] Bing Yin,*[a] Yichen Sun,[b] Zhenxing Wang,*[b] Zhongwen Ouyang,[b] Wenyuan Wang[a] and Shengli Gao[a]

[a] *Key Laboratory of Synthetic and Natural Functional Molecule Chemistry of Ministry of Education, College of Chemistry and Materials Science, Northwest University, Xi'an, Shaanxi 710069, PR China. *E-mail: sanpingchen@126.com; rayinyin@nwu.edu.cn*

[b] *Wuhan National High Magnetic Field Center, Huazhong University of Science and Technology, Wuhan 430074, China. *E-mail: zxwang@hust.edu.cn*

[c] *College of Chemistry and Chemical Engineering, Baoji University of Arts and Sciences, Baoji 721013, China*

‡ These authors have equal contribution to this work.

Table S1 Crystallographic Data for **1** and **2.**

Compound	**1**	**2**
Empirical formula	$C_{26}H_{22}CoS_2N_{12}O_2$	$C_{26}H_{22}NiS_2N_{12}O_2$
Formula weight	657.61	657.39
Temperature	296(2) K	296 K
Crystal system	Orthorhombic	Orthorhombic
space group	$Pca2_1$	$Pca2_1$
a (Å)	17.246(7)	17.119(2)
b (Å)	9.876(4)	9.8597(13)
c (Å)	16.480(7)	16.463(2)
α (°)	90	90
β (°)	90	90
γ (°)	90	90
V (Å^3)	2806.9(19)	2791.8(7)
Z	4	4
F(000)	1348.0	1352.0
Goodness-of-fit on F^2	0.913	1.049
Final R indices [I>2sigma(I)]	$R1 = 0.0923$ $wR_2 = 0.2039$	$R1 = 0.0460$ $wR_2 = 0.1173$
R indices (all data)	$R1 = 0.1992$ $wR_2 = 0.2491$	$R1 = 0.0605$ $wR_2 = 0.1279$
CCDC	1458082	1456495

Table S2 Selected bond lengths (Å) and angles (°) for **1** and **2**.

1			
Co(1)-N(1)	2.226(11)	N(11)-Co(1)-N(12)	178.3(5)
Co(1)-N(5A)	2.212(10)	N(11)-Co(1)-N(6)	87.7(5)
Co(1)-N(6)	2.181(12)	N(12)-Co(1)-N(6)	91.3(4)
Co(1)-N(10B)	2.219(10)	N(11)-Co(1)-N(6)	91.3(4)
Co(1)-N(11)	2.059(12)	N(11)-Co(1)-N(5A)	88.5(4)
Co(1)-N(12)	2.076(12)	N(12)-Co(1)-N(5A)	90.1(5)
N(11)-Co(1)-N(10B)	91.6(4)	N(6)-Co(1)-N(5A)	87.5(4)
N(5A)-Co(1)-N(10B)	179.2(5)	N(12)-Co(1)-N(10B)	89.8(4)
N(11)-Co(1)-N(1)	93.0(5)	N(6)-Co(1)-N(10B)	91.7(4)
N(12)-Co(1)-N(1)	88.0(4)	N(6)-Co(1)-N(1)	178.4(5)
N(10B)-Co(1)-N(1)	89.7(4)	N(5A)-Co(1)-N(1)	91.1(4)
Symmetry codes: A = -0.5+x, 1-y, z; B =0.5+x, 2-y, z			
2			
Ni(1)-N(1)	2.170(4)	N(11)-Ni(1)-N(12)	178.3(5)
Ni(1)-N(6)	2.167(4)	N(12)-Ni(1)-N(5C)	88.24(15)
Ni(1)-N(11)	2.030(4)	N(6)-Ni(1)-N(5C)	89.00(14)
Ni(1)-N(12)	2.036(4)	N(11)-Ni(1)-N(1)	89.20(17)
Ni(1)-N(5C)	2.171(4)	N(12)-Ni(1)-N(1)	89.86(16)
Ni(1)-N(10D)	2.176(4)	N(6)-Ni(1)-N(1)	178.56(16)
N(5C)-Ni(1)-N(1)	91.32(15)	N(11)-Ni(1)-N(10D)	89.47(16)
N(11)-Ni(1)-N(12)	178.8(2)	N(12)-Ni(1)-N(10D)	91.18(15)
N(11)-Ni(1)-N(6)	92.20(16)	N(6)-Ni(1)-N(10D)	91.38(15)
N(12)-Ni(1)-N(6)	88.74(16)	N(5C)-Ni(1)-N(10D)	179.30(18)
N(11)-Ni(1)-N(5C)	91.10(16)	N(1)-Ni(1)-N(10D)	88.29(15)
Symmetry codes: C = 0.5+x, 1-y, z; D = -0.5+x, -y, z			

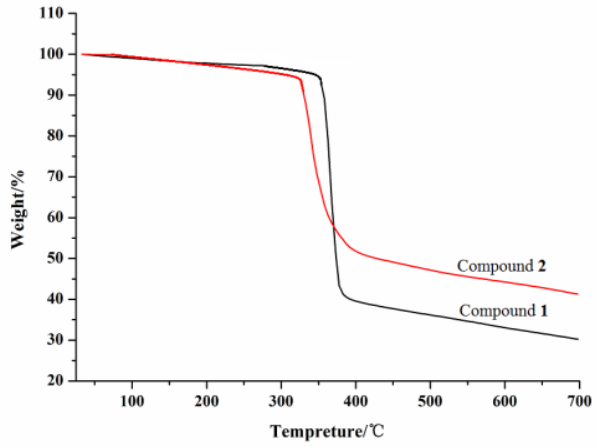

Fig. S1 TGA curves of **1** (black) and **2** (red) under dry N_2 atmosphere.

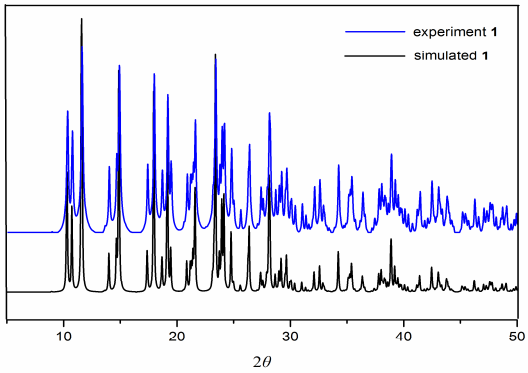

Fig. S2 Experimental XRPD and calculated XRPD of $\{[Co(3,3'\text{-}Hbpt)_2(SCN)_2]\cdot 2H_2O\}_n$ (**1**).

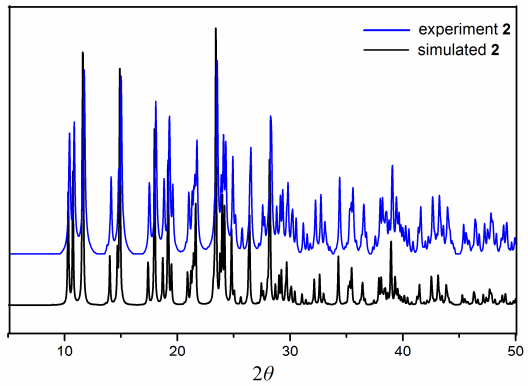

Fig. S3 Experimental XRPD and calculated XRPD of $\{[Ni(3,3'\text{-}Hbpt)_2(SCN)_2]\cdot 2H_2O\}_n$ (**2**).

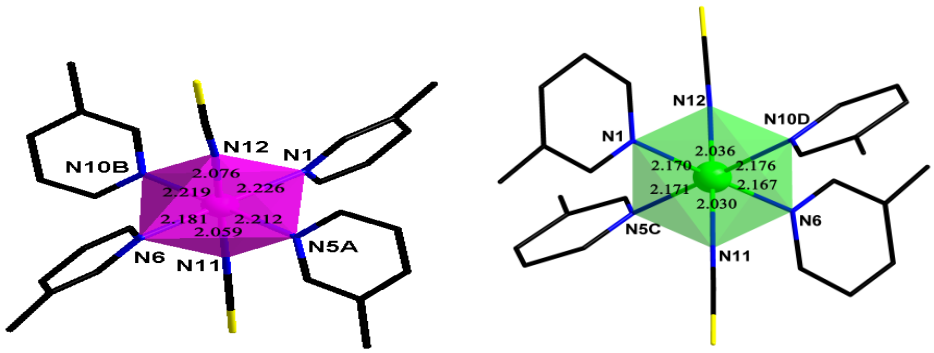

(a) (b)

Fig. S4 View of the metal coordination polyhedron of **1** and **2** showing the tetragonally distorted geometry of the metal atoms. Cobalt, nickel and nitrogen atoms are represented with purple, green and blue colors, respectively.

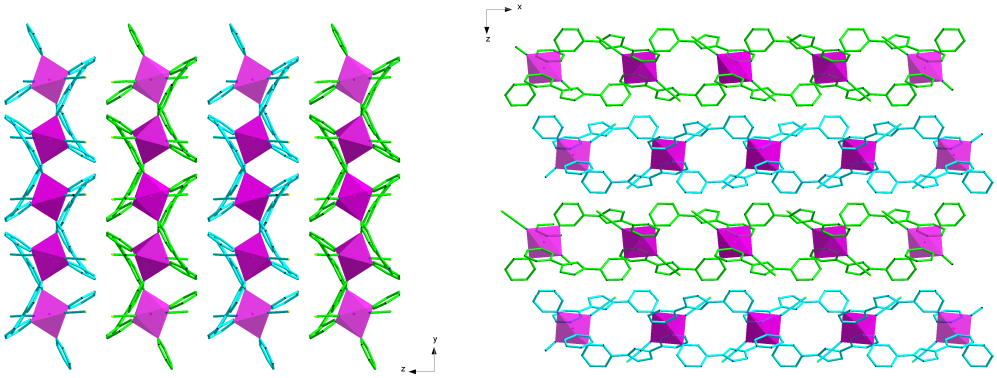

(a) (b)

Fig. S5 View of the 3D framework along the *x* axis (a) and *y* axis (b). The H_2O guests are omitted.

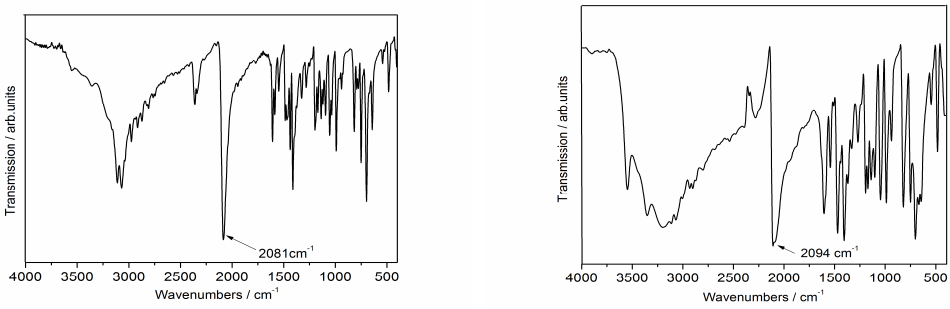

(a) (b)

Fig. S6 IR spectrum for **1** and **2.**

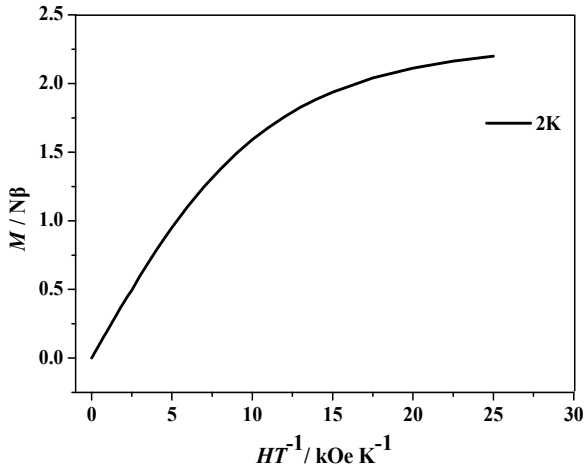

Fig. S7 Experimental *M* versus *H*/*T* plots of **2**.

Table S3 The contributions of the components of the ground Quartet spin eigenstates in the ground (KD_0) and first excited Kramers doublets (KD_1) of (%)[a]

		KD_0-1	KD_0-2	KD_1-1	KD_1-2
1	$\left\|+\frac{1}{2}\right\rangle$	60.61/64.33[b]	/	2.76/3.15	2.40/2.74
	$\left\|-\frac{1}{2}\right\rangle$	/	60.61/64.33	2.40/2.74	2.76/3.15
	$\left\|+\frac{3}{2}\right\rangle$	2.75/3.30	1.24/1.37	/	80.48/82.50
	$\left\|-\frac{3}{2}\right\rangle$	1.24/1.37	2.75/3.30	80.48/82.50	/
1'	$\left\|+\frac{1}{2}\right\rangle$	60.78/65.62	/	2.69/2.93	2.20/2.42
	$\left\|-\frac{1}{2}\right\rangle$	/	60.78/65.62	2.20/2.42	2.69/2.93
	$\left\|+\frac{3}{2}\right\rangle$	2.53/2.74	1.24/1.46	/	80.82/83.54
	$\left\|-\frac{3}{2}\right\rangle$	1.24/1.46	2.53/2.74	80.82/83.54	/
1"	$\left\|+\frac{1}{2}\right\rangle$	58.84/63.45	2.14/2.41	2.80/3.08	1.45/1.48
	$\left\|-\frac{1}{2}\right\rangle$	2.14/2.41	58.84/63.45	1.45/1.48	2.80/3.08
	$\left\|+\frac{3}{2}\right\rangle$	1.90/2.06	1.19/1.34	/	81.32/84.12
	$\left\|-\frac{3}{2}\right\rangle$	1.19/1.34	1.90/2.06	81.32/84.12	/

[a] only the contributions larger than 1% are shown here; [b] The results from CASSCF are at the left side of "/" and the results from NEVPT2 are at the right side of "/".

Table S4 The contributions of 5 metal 3*d* orbitals to the active orbitals of CASSCF wavefunction (%).

	d_{z2}	d_{xz}	d_{yz}	d_{xy}	d_{x2-y2}
ϕ_1	2.3	2.4	29.5	27.6	37.1
ϕ_2	13.9	25.6	1.8	50.2	7.3
ϕ_3	75.0	21.2	0.0	0.5	2.2
ϕ_4	6.9	47.8	6.1	18.9	15.7
ϕ_5	0.5	0.1	58.3	1.0	34.4

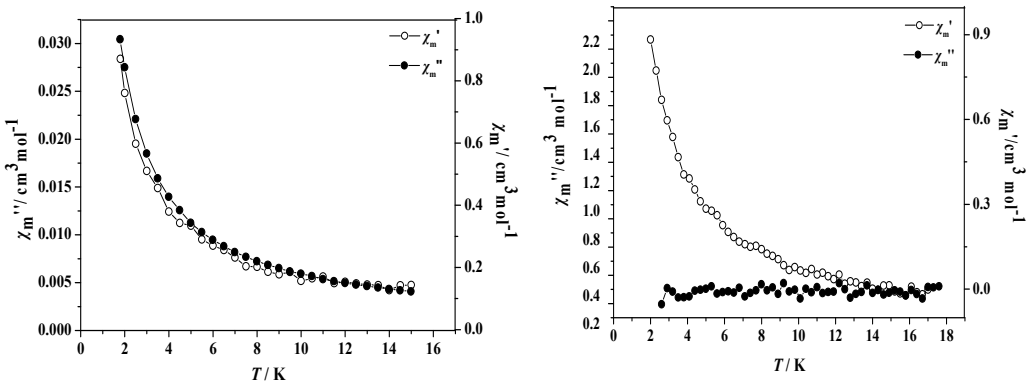

(a) (b)

Fig. S8 Temperature dependence of the in-phase and out-of phase ac susceptibility signals for **1** and **2** under 0Oe dc field.

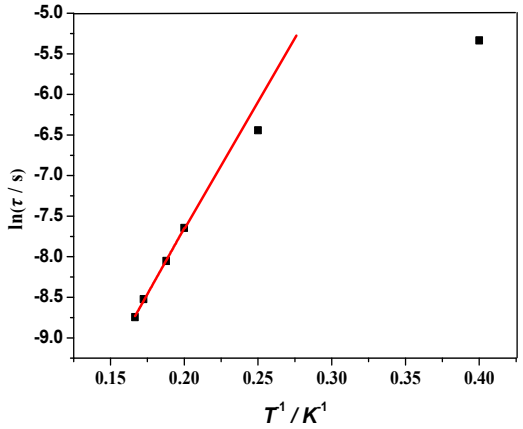

Fig. S9 Magnetization relaxation time, lnτ vs. T^{-1} plot under 1.5 kOe dc field for **1**. The solid line is fitted with the Arrhenius law.

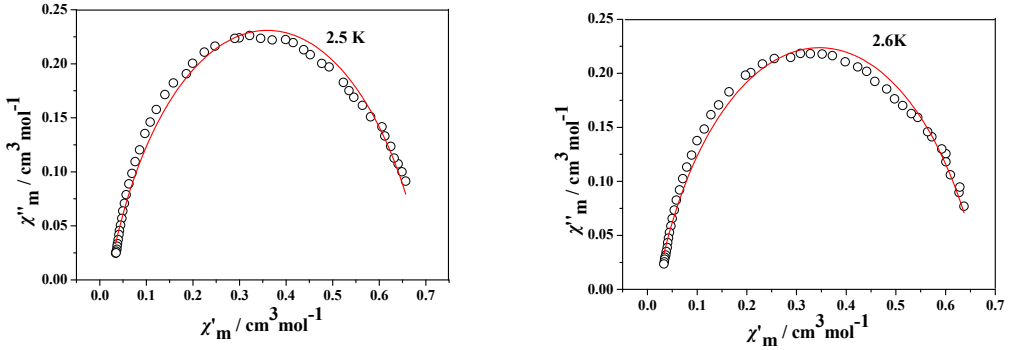

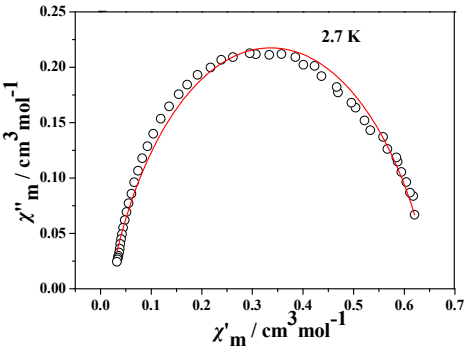
2.7 K
χ''m / cm3mol-1
χ'm / cm3mol-1

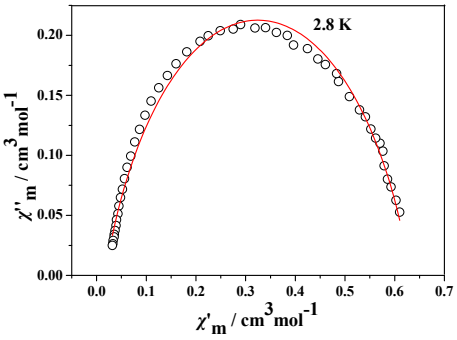
2.8 K
χ''m / cm3mol-1
χ'm / cm3mol-1

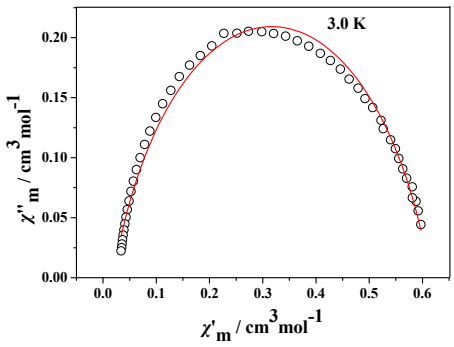
3.0 K
χ''m / cm3mol-1
χ'm / cm3mol-1

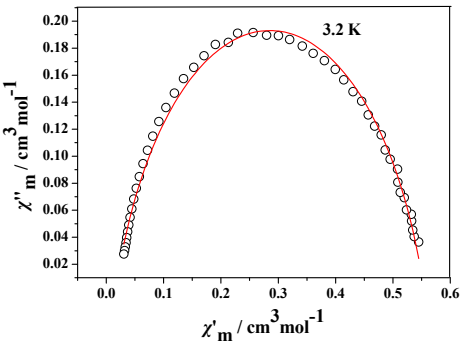
3.2 K
χ''m / cm3mol-1
χ'm / cm3mol-1

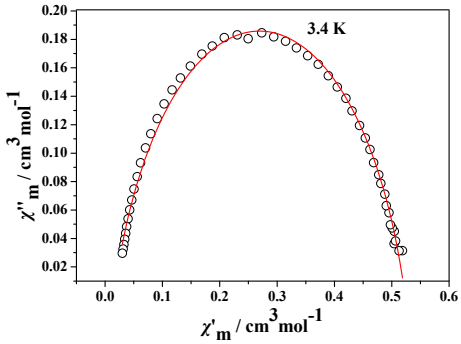
3.4 K
χ''m / cm3mol-1
χ'm / cm3mol-1

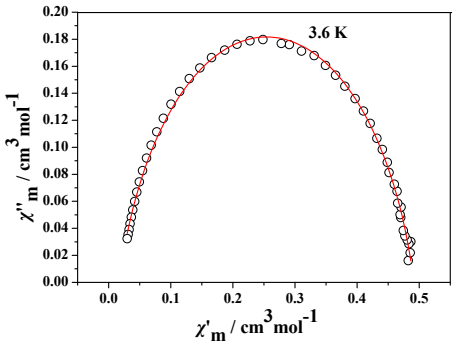
3.6 K
χ''m / cm3mol-1
χ'm / cm3mol-1

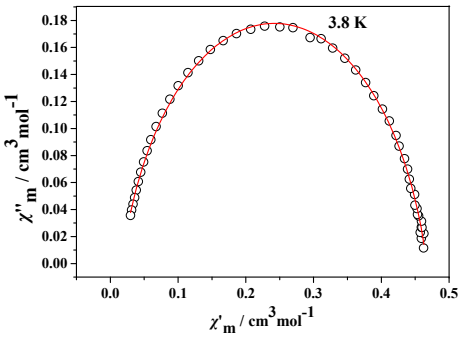
3.8 K
χ''m / cm3mol-1
χ'm / cm3mol-1

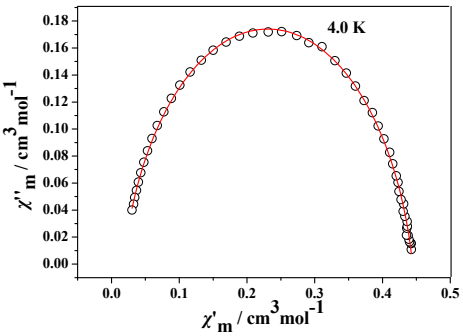
4.0 K
χ''m / cm3mol-1
χ'm / cm3mol-1

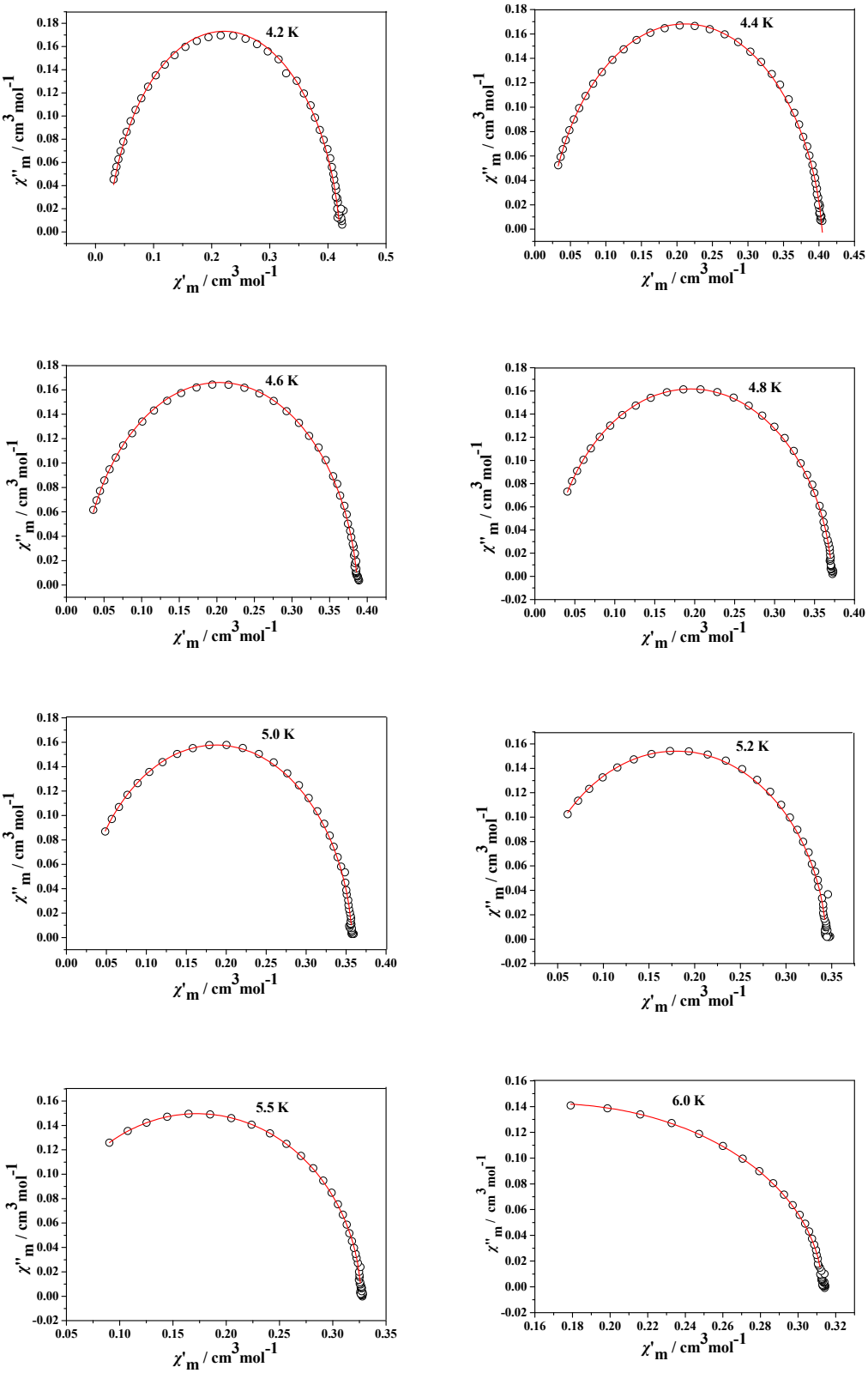

Fig. S10 Simulations of dynamical susceptibility $\chi(\omega)$ ranging from 2.0 to 10 K in a Cole-Cole diagram of **1**. Red lines were performed using the sum of two modified Debye functions with the fitting parameters in Table S3.

The magnetic susceptibility data were described by the modified Debye functions:

$$\chi'(\omega) = \chi_S + (\chi_T - \chi_S)\frac{1+(\omega\tau)^{1-\alpha}\sin(\frac{\pi}{2}\alpha)}{1+2(\omega\tau)^{1-\alpha}\sin(\frac{\pi}{2}\alpha)+(\omega\tau)^{(2-2\alpha)}}$$

$$\chi''(\omega) = (\chi_T - \chi_S)\frac{(\omega\tau)^{1-\alpha}\cos(\frac{\pi}{2}\alpha)}{1+2(\omega\tau)^{1-\alpha}\sin(\frac{\pi}{2}\alpha)+(\omega\tau)^{(2-2\alpha)}}$$

$$\chi''_{\omega=\tau^{-1}} = (\chi_T - \chi_S)\frac{\cos(\frac{\pi}{2}\alpha)}{2+2\sin(\frac{\pi}{2}\alpha)} = \frac{1}{2}(\chi_T - \chi_S)\tan\frac{\pi}{4}(1-\alpha)$$

Table S4 Relaxation fitting parameters from Least-Squares Fitting of $\chi(\omega)$ data of **1**.

T(K)	$\Delta\chi_1$ (cm^3mol^{-1})	$\Delta\chi_2$ (cm^3mol^{-1})	α
2.5	0.70081	0.01876	0.24212
2.6	0.67483	0.01803	0.23874
2.7	0.66576	0.01710	0.23865
2.8	0.63165	0.01707	0.222928
3.0	0.61445	0.0192	0.21988
3.2	0.55446	0.01619	0.20775
3.4	0.52286	0.01567	0.1948
3.6	0.49155	0.01698	0.16789
3.8	0.4667	0.01744	0.14765
4.0	0.44441	0.0174	0.12918
4.2	0.42073	0.021	0.09091
4.4	0.40442	0.01808	0.08787
4.6	0.38717	0.01921	0.06538
4.8	0.37216	0.01766	0.05825
5.0	0.35767	0.01635	0.05009
5.2	0.34442	0.01505	0.04209
5.5	0.32656	0.0184	0.01864
6.0	0.31283	0.02186	0.01387

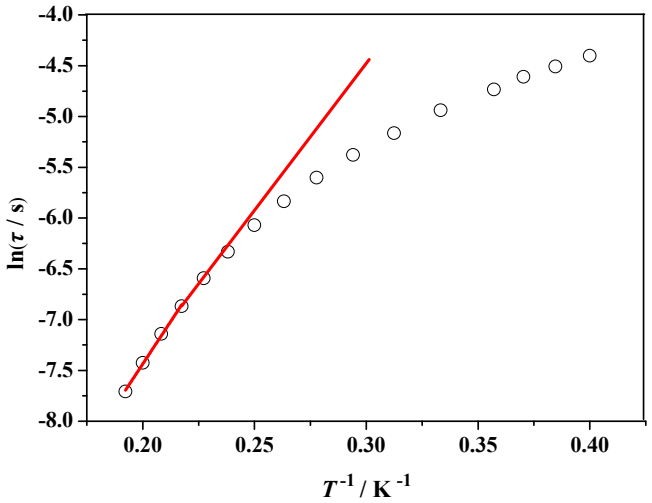

Fig.S11 Relaxation time of the magnetization *ln(τ)* vs T^{-1} plot under the 1.5 KOe applied field for **1**.

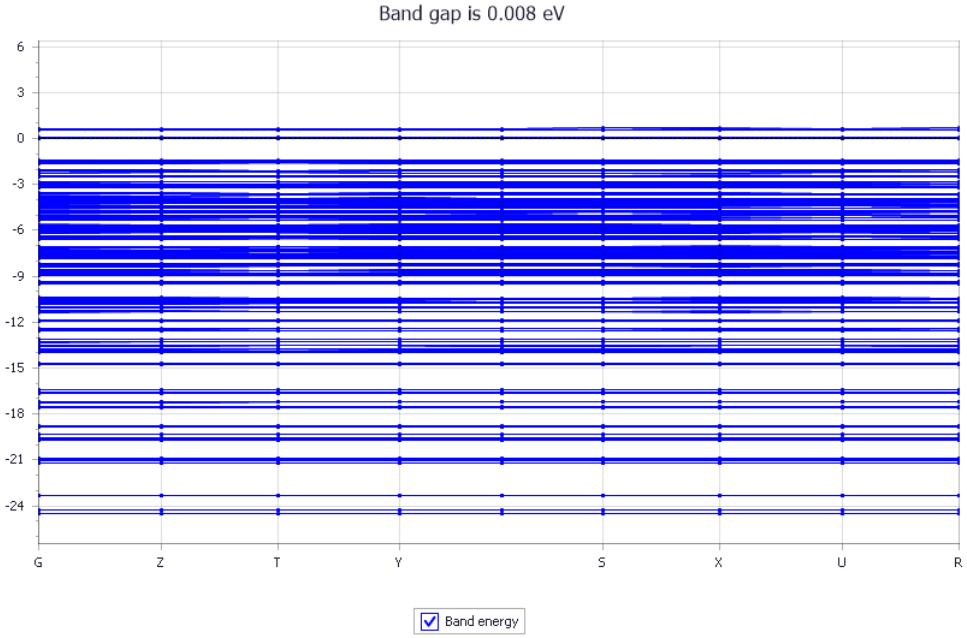

Fig. S12 The simulated band gap of compound **1**, the calculated value is 0.008 eV. (The Fermi level is set at 0 eV).

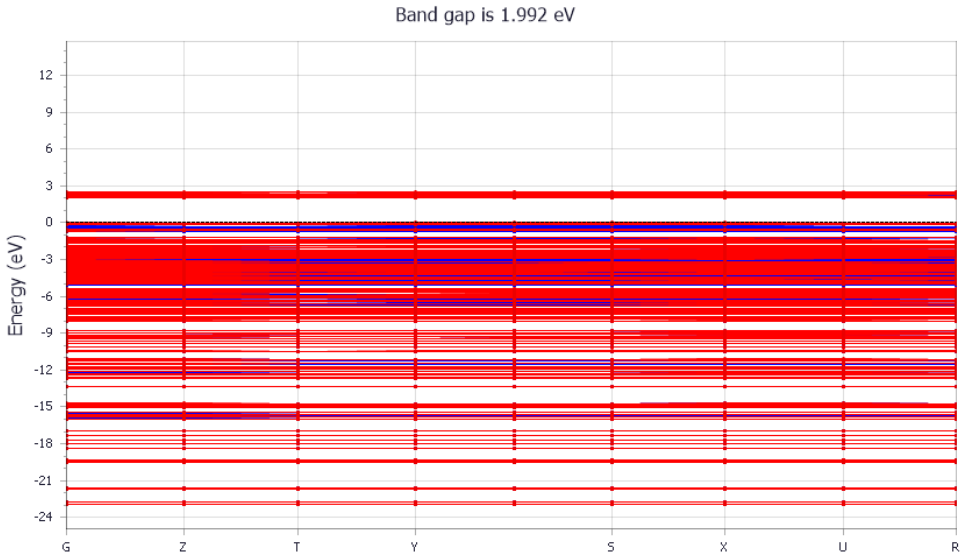

Fig. S13 The simulated band gap of compound **2**, the calculated value is 1.992 eV. (The Fermi level is set at 0 eV).